Searching for solar-like interannual to bidecadal effects on temperature and precipitation over a Southern Hemisphere location

Teresita Heredia[1,2], Flavia M. Bazzano[1,2,3], Rodolfo G. Cionco[4,5], Willie Soon[6], Franco D. Medina[1], and Ana G. Elias,[1,2]

(1) Laboratorio de Física de la Atmósfera, Facultad de Ciencias Exactas y Tecnología, Universidad Nacional de Tucuman, Av. Independencia 1800, 4000 Tucuman, Argentina

(2) INFINOA (CONICET-UNT), Tucuman, Argentina

(3) Laboratorio de Construcciones Hidráulicas, Dpto. de Construcciones y Obras Civiles, Facultad de Ciencias Exactas y Tecnología, Universidad Nacional de Tucumán

(4) Comisión de Investigaciones Científicas, Buenos Aires (CICPBA) y Grupo de Estudios Ambientales, UTN, Colón 332, San Nicolás, Bs As.

(5) Consejo Nacional de Investigaciones Científicas y Técnicas, CONICET

(6) Center for Environmental Research and Earth Sciences (CERES), Salem, MA 01970, USA

Note: *This is a pre-print version of this article. The typeset version is published at: J. Atmos. Sol.-Terr. Phys., Vol. 193, 15 October 2019, 105096.* https://doi.org/10.1016/j.jastp.2019.105094

Abstract

Precipitation and temperature over Tucuman (26.8°S, 65.2°W), a province located in the Northwestern region of Argentina, is analyzed for the interval 1889-2018 in search of any plausible statistical associations with impacts and responses from solar variability . The aim of the study was to contribute data to the controversial issue of climate variations in response to both anthropogenic and natural forcings. The long-term behavior of Tucuman climatic series involves overall warming and augmented precipitation tendencies, possibly linked to the increasing greenhouse gases concentration or even other local man-made factors like increasing urbanization. In addition, we identified sporadic ~4 and ~8-year periodicities, and a ~20-year oscillation after the 1950-1960's. Based on the physical hint that bidecadal periodicities detected in climate parameters are probably not linked to the solar 11-year-like irradiance cycles, we expand our scope of investigations to include another effect which has been recently considered in the dynamics of large rivers as "the planetary hypothesis of the solar cycles". This new hypothesis supposes that the barycentric dynamics of the Sun could be involved in modulations

of the intrinsic solar magnetic and radiative output cycles and therefore Earth-bound climatic responses. Thus, we present a wide-ranging statistical analysis of correlation, cross spectrum, and coherence between Tucuman's climatic series and solar orbital parameters, including also the analysis of hemispheric mean temperatures. Our results show significant coherence at the ~20-year cycle, which is clearly present in the Sun's barycentric dynamic that could in turn be linked to some features of the quasi-decadal solar activity variations.

Keywords

solar forcing; barycentric dynamics; greenhouse gases; climate

1. Introduction

Some features of the Sun are not yet completely understood, among which are the regularities and irregularities of the solar magnetic activity cycles. In order to understand these phenomena, theories have been developed that resulted in models capable of reproducing some aspects of solar activity variations that cover timescales from interannual to bimillennia or longer timescales.

The most promising and fruitful direction in the theoretical "framing" of these observed solar magnetic activity features is the magnetohydrodynamic dynamo theory (see for example the review of Priest, 2011). The study of solar magnetic variability, including prolonged activity minima can be cast in a solar dynamo theory (Brandenburg et al., 2017). Despite the progress in this field, it is clear that both the actual triggering and stopping mechanisms of solar cycles are still far from being understood; moreover, an external parametric force is needed to produce magnetic cyclicity and long-term variations. In this sense, Cionco and Soon (2015) proposed an optimal Sun-Planets Interaction (SPI) framework that can account for the timing of so-called solar activity Grand Minima (i.e., Usoskin et al., 2016) for the past 1000 years or so. Stefani et al. (2019) focuses more on the shorter term (i.e., interannual, decadal to bidecadal timescales) modulation mechanism, via planetary tidal synchronization, that involves the helicity parameters of the Tayler-Spruit dynamo equations.

Solar activity cycles are one of the fundamental "features" in the Sun-Earth relationship. Therefore, it is priority for geophysics, in a wide sense, and especially for Earth climate dynamic studies to understand and forecast solar variability (Jones et al., 2012, Soon et al., 2015). Solar cyclic changes as irradiance variations following the orbital-Milankovitch forcing (Cionco and Soon, 2017) or other plausible mechanisms related to planetary movement are increasingly being explored (see e.g., Sun et al., 2017).

The solar barycentric motion (SBM, formerly known as solar inertial motion) result from a complex model of *N*-body interactions in the Solar System (Cionco and Pavlov, 2018). The Sun

moves around the center of mass of the solar system, called the barycenter. This movement mainly reflects the orbits of the two largest giant planets: Jupiter and Saturn, whose orbital periods are ~ 11.9 years and ~ 29.5 years respectively, and which constitute the 93% of the total planetary mass.

Several authors have associated the SBM with climatic and solar activity series (Jose, 1965; Charvatova, 2000; Leal-Silva and Velasco Herrera, 2012 Scafetta, 2010; Cionco and Compagnucci, 2012; McCracken et al., 2014; Cionco and Abuin, 2016; Okhlopkov, 2016; Sun et al., 2017; McCrann et al., 2018). However, other authors criticize the statistical methods adopted and the significance of some of the results (Cameron and Schussler, 2013; Holm, 2014, 2015). They argue that in many cases the observed coherence, despite being high, is not significant and lacks physical mechanism that can adequately explain this planetary hypothesis.

The hypothesis of a gravitational influence of the planets in the solar magnetic cycle is an old idea (reviewed by Cionco and Compagnucci, 2012) showing associations in several cycles, such as the quasi-decadal variation and ~20, ~30 and ~60-year quasi-oscillations, based on correlations between the movement of the Sun around the barycenter and its sunspots. This planetary hypothesis is a new perspective on the Sun-climate issue, even though according to the IPCC reports (IPCC, 2014) the influence of the Sun on Earth's climate since the industrial era, in terms of radiative forcing is very small compared to the radiative forcing due to the anthropogenic greenhouse gases increase. Some works connect the discharge of rivers with the planetary dynamics (Zanchettin et al., 2008; Antico and Krohling, 2011; Cionco and Abuin, 2016) showing significant correlations between them and suggesting a possible physical mechanism that relates planetary movements, internal processes of the Sun and rivers' dynamics on Earth.

In general, it is assumed that solar-climate interaction is due to solar irradiance forcing and this specific proposal has been reviewed in Soon (2009) and Soon et al. (2014). However, there are other mechanisms linked to solar radiations in a broader electromagnetic frequency range, like ultraviolet solar radiation, and to cosmic rays or solar wind variations that could involve the modulation of cloud covers and other cloud properties (Kirkby, 2007; Mendoza et al., 2016). Other still unknown space weather and gravitational mechanisms may exist. Furthermore, climate response to changes in solar irradiance may happen at different time scales, which can be masked if there are strong inherent oscillations in a solar parameter for example and not in climate, or vice versa. Thus, in order to find a relationship between climate and a given solar periodicity, the strong solar activity periodicity, or quasi-periodicity, may be filtered out applying an 11-year running mean to the solar parameter before performing the corresponding analysis, so that the strong 11-year cycle can be removed (Gil-Alana et al., 2014). Such an important separation of physical timescales and mechanisms owing to distinct local and regional land-air-ocean responses has been emphasized by Soon (2009). Another point to consider is that sea surface temperature is affected by changes in the deep oceans presenting variations on time

scales from one to several decades, so the use of land surface temperatures may be a better option to analyze (Gil-Alana et al., 2014; Sfica et al., 2018).

There are now sophisticated methods and models to detect correlation or causality. For example, slow feature analysis (SFA) (Wiskott, 2003) is a statistical technique to extract the driving force information behind a data series, assuming this driving force is a slowly changing mechanism. Wang et al. (2017) analyzed the Central England Temperature (CET) dataset, using the SFA technique and wavelet analysis (see the pioneering study by Baliunas et al. 1997 that essentially found similar multi-scale oscillations including 7.5 yr and 14.4 yr scales also reported by Wang et al. 2017). They detected a 3.36-year cycle and a 22.6-year cycle that seem to be connected to the El Niño Southern Oscillation and the Hale sunspot cycle, respectively. They also modeled and speculated that these driving forces are modulated in amplitude by a long periodic signal of millennial timescale. They further speculated that this millennial signal may be an impact of greenhouse gases. Scafetta and colleagues (Scafetta and West, 2007; Scafetta, 2010, 2012, 2014, 2016) consider this millennial scale period to be partly caused by solar variations associated to the planetary hypothesis and argue that solar/astronomical effects likely count at least 50% of the observed warming. This conclusion derives from various considerations, and some of them include the analysis of the temperature of the past at least up to the medieval times that Wang et al (2017) do not address. However, as stated by Wang et al. (2017): “here we prefer to regard it as the GHG -greenhouse gases- signal for the physical energy of the climate system”.
In this work, we propose to study the statistical inter-relationships between Sun and climatic variations within the spectral frequency domain in which we believe the physical nature of the complexity can be better revealed and hence understood. We adopt relatively simple techniques, mainly correlations combined with wavelet cross spectra, paying attention to the statistical significance estimations and modified degrees of freedom when smoothing is applied to the time series analyzed.

As mentioned by Kristoufek (2017), and many other authors, the detection of solar-climate association has many issues. Among them, the methodology used which can strongly affect the results, cyclical and trend components playing important roles, possible non-linear interactions playing also key roles, and time variation of the sought relationship. To overcome some of these issues, Kristoufek (2017) uses continuous wavelet coherence analysis, which we also use in conjunction to its Fourier counterpart and a correlation analysis. He shows that the relationship between *Rz* and temperature has been “disturbed” by CO2 since the 1960s. Once this relationship is taken into account by filtering it, they obtain significant coherence between *Rz* and global and hemispheric temperatures at ~20-year periodicity. They support their results with the Granger causality tests (Granger, 1969), which, as already mentioned, involve more complex statistics.

We choose to follow simpler statistics, which in our opinion allow for clearer and more direct interpretations.

2. Data

Annual-mean solar and climatic data series were used in this study in order to detect a possible association between solar and climate variations at a particular station in the Southern Hemisphere: Tucuman (26.8°S, 65.2°W), at 481 meters above sea level, located in the Northwestern region of Argentina.

Tucuman has one of the longest climatic series in Argentina, and the longest in the Northwestern region of the country without data gaps. In addition, in the case of the precipitation time series it can be considered as representative of the Northwestern region which extends between 22° and 29°S and between 63° and 68°W (Heredia and Elias, 2013).

Data since 1911 correspond to the Estacion Experimental Agroindustrial Obispo Colombres (EEAOC) located in El Colmenar, Tucuman. Prior to 1911 they belong to a location 4.6 km apart. This first period of data covers 1889 through 1935 so, the simultaneous 1911-1935 period was used in order to obtain homogeneous time series in both cases (Kenning, 1963; Minetti, 1991; Minetti and Vargas, 1997) covering from 1889 until present.

Solar data includes:

* SBM obtained from the ephemerides EPM2017H (Cionco and Pavlov, 2017), which can be downloaded from https://doi.pangaea.de/10.1594/PANGAEA.882534, and are fully explained with a detailed description and equations used in their calculations in Cionco and Compagnucci (2012). We use the magnitude of the barycentric position of the Sun, r, the modulus of the solar orbital angular momentum, L, and its variation (the so called solar "torque"), dL/dt.

* Sunspot number, *Rz*, obtained from WDC-SILSO, Royal Observatory of Belgium, Brussels (available at from http://www.sidc.be/silso/datafiles).

* Total Solar Irradiance (TSI) reconstruction based on the model by Lean and described by Coddington et al. (2015) (available at http://lasp.colorado.edu/home/sorce/data/tsi-data/#historical_TSI), which corresponds to the NRLTSI (Naval Research Laboratory Total Solar Irradiance) reconstruction, one of the two key datasets of TSI historical records. The other one is SATIRE (spectral and total irradiance reconstruction). NRLTSI is based on solar proxies and observations of TSI, being thus an empirical TSI model, while SATIRE is a semi-empirical model since it uses calculated intensities and proxies generated from model solar atmospheres. Both results compared very well in the time scales of interest in this work (Matthes et al., 2017).

Climatic data includes:

* mean temperature and total precipitation over Tucuman obtained from the South American Climatic Laboratory and correspond to annual data for the period 1889 – 2018,

* Northern Hemisphere (NH) and Southern Hemisphere (SH) mean temperature data sets developed by the Climatic Research Unit (CRU, University of East Anglia) together with the

Hadley Center (UK Met Office), which correspond to anomalies with respect to the average of the 1961-1990 period (available at https://crudata.uea.ac.uk/cru/data/temperature/), including the following:

- CRUTEM4 NH and SH land air temperature (Jones et al., 2012),

- HadSST3 NH and SH sea surface temperature (Kennedy et al, 2011a, 2011b),

In all studied cases we considered the period 1889-2018 that is the longest period available for Tucuman data. Figure 1 shows solar annual data, and Figure 2 Tucuman series and hemispheric temperatures. The quasi-decadal variability of TSI and Rz is clearly noticed in Figure 1(a), with cycles even tending to be lower in amplitude than one or both of the adjacent odd cycles, and rise time to the maximum within a given cycle faster than the corresponding declining phase (Russell et al., 2016). Both features, "alternation" in cycle's intensity and phase asymmetry, imprint certain characteristics to the spectrum which will be discussed later in this work. The ~20-year cycle noticed in Sun's orbital data and shown in Figure 1(b), which we will also call bi-decadal cycle, presents some asymmetry and amplitude variations, although not as systematic as in quasi-decadal cycle case. Regarding climatic series, a strong short-term inter-annual variation can be noticed that is totally absent in solar data and which masks any probable decadal or bi-decadal oscillation, together with an almost steady increasing trend, especially in global and hemispheric temperature data.

3. Trend estimations

Trends in time series are usually filtered out before applying spectral studies. These trends, however, can imply a stronger variation than those due to periodical oscillations. In climatic series, trends beginning in the 1800's are commonly linked to increasing greenhouse gases concentration. Figure 3 shows the global CO_2 mixing ratio obtained from the Goddard Institute for Space Studies (GISS) since 1850, together with a linear and a quadratic fitted trend. The quadratic fit shows a better adjustment, as can be deduced from the correlation coefficients shown in the graph.

Linear and quadratic trends for each climatic series were estimated with the method of least squares, having first tested that they are all normally distributed with the Kolmogorov-Smirnov test at the 5% significance level. The expected change per year and for the 130-year period, from 1889 to 2018, was calculated based on these trends. A negligible difference was observed for the total variation between the linear and the quadratic assessments. Table 1 shows the total increase during the 130-year period assessed from the quadratic fit, and the increase per year obtained with the linear fit, which multiplied by 130 is almost equal to the total increase. These values will be later compared with variations expected from a ~20-year periodicity.

4. Power spectrum analysis

Original climatic time series were detrended with a quadratic fit, followed by a wavelet transform (WT) that is able to detect periodicities with amplitude and significance that may change in time, a condition mostly common in climatic and solar data series.

WT was calculated using the computational algorithm of Torrence and Compo (1998). The Morlet wavelet commonly used in climatic series analysis was chosen, given by

$$\psi_o(\eta) = \pi^{-1/4} e^{i\omega_o \eta} e^{-\eta^2/2} \quad (1)$$

where ω_o is a dimensionless frequency taken as 6, which allows a good balance between time and frequency localization (Grinsted et al., 2004). Given the time series length, WT provides significant results for periodicities shorter than ~45 years.

Figure 4 shows WTs of climatic data series. Significant peaks appear sporadically at periodicities between ~8 and ~2-4 years in both Tucuman series and in SH temperatures. Also a ~13-year in the case of SH land temperature, and a ~20-year cycle in the cases of Tucuman precipitation and SH sea temperature, are detected as significant. The Northern Hemisphere only presents as significant a ~4-year periodicity but very sporadically. We will focus in this work only on the ~20-year cycle which appears as significant in Tucuman precipitation after the 1960's, and also in Tucuman temperature even though not statistically significant. In the case of SH sea temperature is significant before the 1940's.

The fact that NH temperatures do not present the bi-decadal variation and that in the case of Tucuman temperature appears faintly but with no statistical significance, may point out that this cycle is probably more linked to sea characteristic than to land. This could be concluded considering that the Southern Hemisphere has 80% of its surface covered by water while the Northern Hemisphere has 60%, and that Tucuman precipitation is directly linked to air masses coming from the Atlantic Ocean (Seluchi et al. 2003; Heredia and Elias, 2013).

Figure 5 shows WTs of solar parameters. Here the ~11-year period in *Rz* and TSI, and the ~20 year period in *r* and *L* are very well defined. The WT of d*L*/d*t* (not shown) is almost identical to that of *L*.

5. Cross spectrum and coherence

To statistically determine a possible association between solar variation and climatic series of Tucuman, the cross wavelet transform (XWT) and the wavelet coherence (WTC) between them were assessed, considering their ability to detect association in frequency (or periodicity) domain that may change in time in a rather simple way. XWT, equivalent to the Fourier cross power spectrum, measures periods with high common power, i.e. when both time series have a common oscillation in terms of frequency. It also gives information on the phase relationship through arrows, which points right when both series are in-phase, left when they are in anti-

phase, straight down when the second series leads the first by 90°, and so on. WTC corresponds to the square of the cross-spectrum normalized by the individual power spectra, thus giving a quantity between 0 and 1, identifying frequency bands that have a common variation in both series, even if the power at the corresponding frequency in any of the two series is low. It measures the correlation between two time series in terms of frequency. As in the case of Fourier coherence, this coherence is identically one at all times and scales if it is estimated with the raw spectrum estimations. This problem is solved by smoothing the cross-spectrum before normalizing, so care should be taken regarding the smoothing procedure. For this analysis we used the software developed by Aslak Grinsted (available at http://www.glaciology.net/wavelet-coherence/) (Grinsted et al., 2004).

Figure 6 shows XWT and WTC between *r* and both Tucuman detrended series. Similar plots (not shown) are obtained for L and d*L*/d*t*. A clear common power is noticed for a ~20-year quasi-periodicity during the whole period, but with different phases. However, there is significant coherence only after 1960's in the case of precipitation with in-phase variation. A 90° offset is observed in the case of Tucuman temperature but it does not reach the 95% confidence level.

In the case of hemispheric land temperatures, shown in Figure 7, SH presents XWT and WTC similar to Tucuman temperature, but with a significant phase difference slightly smaller than 90°. In the case of NH the ~20-year quasi-periodicity appears as significant in XWT and WTC during the whole period with a clear in-phase common variation, even though this periodicity has no significance in NH land WT (see Figure 4e). XWT and WTC for hemispheric sea temperatures, shown in Figure 8, indicate also a significant ~20-year quasi-periodicity where the coherence has shifted to the period prior to 1960's in the case of SH, and it is more limited in time, around 1960's, for NH.

Figures 9 and 10 depicts XWT and WTC between Tucuman series and TSI, and also *Rz*. XWT is shown only for the case of TSI since it is identical to the case of *Rz*. The common quasi-decadal variation appears in precipitation and temperature, but without coherence at all. This is due to the strong quasi-decadal variation in *Rz* and TSI. On the other hand, the ~20-year quasi-periodicity, even though faint in the cross spectrum, presents significant coherence after 1960's. Hemispheric land and see temperatures (not shown here) present a similar behavior in the sense that a significant common power appears at the quasi-decadal variation, but coherence appears only at the ~20-year quasi-periodicity during a certain period. Coherence is significant in *Rz* case and not TSI, due to a long-term variation in TSI which is not present in climatic series due to detrending procedure. If TSI is also detrended, WTC looks like those corresponding to *Rz*.

The average variation expected for the bi-decadal periodicity in half a cycle can be assessed as twice the corresponding FFT amplitude. This value is listed in Table 1, together with associated annual variation that is the average half cycle variation divided by ten. This variation has a sign during half a cycle, and the opposite during the other half, contrary to the annual variation

expected for the 130-year long-term trend, which is always positive. Something to note is that the annual variations due to the steady trend and due to the bi-decadal cycle are similar in magnitude for each climatic series. However, one is sustained in time while the other is zero on average.

Regarding the statistical significance of the results about coherence between climate records and barycentric dynamics of the sun, the issue seems to be well studied in Scafetta (2018).

6. Correlation analysis

The possible association between solar and climatic data series was also analyzed using correlation analysis. Variations with time scales shorter than decadal were filtered out first by calculating the 11-year running mean of each detrended time series. Correlation coefficients, r_c, listed in Table 2, were assessed then between solar and climatic series.

The confidence level of each correlation coefficient was estimated with the *t* statistic

$$t = \frac{r_c\sqrt{N-2}}{\sqrt{1-r_{c^2}}}\ t = \frac{r_c\sqrt{N-2}}{\sqrt{1-r_{c^2}}} \qquad (2)$$

with *N*-2 degrees of freedom, *df,* where *N* is the number of independent data in each correlated series. In the case of the raw data *N*=130 so *df*=128, but when an 11-year running mean is applied, the independent data is reduced to 130 divided by 11, that is *df*, or (*N*-2) in equation (2), is reduced to 9. In this case t=1.833 for a 95% confidence level, which means that only r_c>0.52 would be statistically significant. As can be noticed from Table 2, any r_c value exceeds this limit. The r_c parameter before and after 1950 was also calculated, considering that before or after ~1940 to ~1960 coherence becomes significant. In these cases, *df* falls to 3 and 4 respectively, and the corresponding limiting values of r_c become 0.80 and 0.74. The only significant correlation coefficient obtained is between Tucuman precipitation and *r* or *L*, after 1950, with r_c=0.76, roughly reaching the 95% confidence level. Figure 12 shows both series and a direct association can be clearly noticed for the second half of the period here analyzed.

7. Combined characteristics of the quasi-decadal solar activity and bi-decadal Sun's motion cycles

As mentioned in Section 2, two noticeable characteristics of TSI and *Rz* decadal variability (Russell et al., 2016) are the following:

(1) even cycles tend to be lower in amplitude than one or both of the adjacent odd cycles, which can appear as ~20-year peak in a power spectrum,

(2) rise time to the maximum within a given cycle is faster than the falling time, which results in power spectrum peaks at quasi-decadal sub-harmonics (Elias and Zossi, 2006).

Regarding the bi-decadal variation of Sun's motion parameters, a slight asymmetry can be noticed in the rising and falling times, even though not as regular as the asymmetry in the solar activity cycle. This asymmetry results, as in the case of TSI and *Rz*, in power spectrum peaks at sub-harmonics of the 20-year cycle, the first of which would be a ~10-year period.

As a way to test how this shows up in XWT and WTC, artificial series were generated with these features. A time series of 11-year periodicity was constructed then with a combination of purely sine waves in such a way that the rising time was set to 4 years and the descending time to 7, and an alternation of tall and short cycles with a difference of 30% in amplitude. A 20-year purely sine series was constructed also with an asymmetry between the rising and falling phases. As can be seen in Figure 12, where XWT and WTC between TSI and *r*, and between their artificial counterparts, the alternation in the quasi-decadal cycle strength together with the asymmetry in the quasi-decadal and bi-decadal cycles, generate the mean behavior characterized by common powers at ~10 and ~20-year cycles, and sporadic significant coherence at ~20-year.

8. Discussion and conclusions

Our results and conclusions can be summarized as follows:

1) Based on WTs of climatic data series, and considering that the Southern Hemisphere has 20% more water than the Northern Hemisphere and that Tucuman precipitation depends, among other variables, on winds coming from the ocean (Seluchi et al. 2003; Heredia and Elias, 2013), it is possible to argue that the ~20-year cycle is probably linked to the conditional characteristics of the sea surface. The damping effect of the oceanic thermal inertia would also contribute to making some climatic parameters more sensitive to slower solar variations as occurs in our case assuming that the bi-decadal cycle is linked to the Sun (Zanchettin et al., 2008; Stefani et al. 2019).

2) An explanation for the coherence at ~20-year quasi-periodicity between solar activity and Sun's orbital parameters, which in turn is influenced by planetary movement, could be purely statistical. We base this argument on the characteristics of their main cycles: the quasi-decadal variation in solar activity, which has alternating maxima, and the bi-decadal cycle in Sun's motion parameters, which has asymmetric rising and falling duration.

3) If one of the reasons for the alternation of tall and short cycles (i.e., the so-called Gnevyshev-Ohl rule of sunspot number cycles; see Tlatov, 2013; Zolotova and Ponyavin, 2015) in solar activity is linked to the Sun's motion around the barycenter, this would provide a physical explanation supporting our statistical result. A possibility would be the explanation for solar activity variations as forced oscillations between solar system planets and the solar dynamo (Yndestad and Solheim, 2017; Stefani et al., 2019).

4) Assuming that there is a real connection between the Sun and climate through the planetary hypothesis, this connection is usually, as it is in this case, detected after filtering out long-term trends in climatic series. According to our results, this trend could represent values similar to those associated to solar effects.

Regarding the coherence and cross spectrum analyses, they may present certain issues since when one of the two records is highly harmonic XWT might yield artificially high power at the corresponding frequency. Scafetta (2018) discuss this issue fully by showing that climatic data indeed significant peaks at periodicities around 20 years. In addition, when certain periodicities do not appear in the whole data period, as is the case for example in Tucuman precipitation, it may lose power in the computed global spectrum.

Something worth mentioning is that that annual mean temperature and total precipitation over Tucuman, shown in Figure 2a, are negatively correlated at multiple frequencies which means that higher temperatures would correspond to lower annual precipitation, something which would be contrary to the Clausius-Clapeyron relation between the atmosphere temperature and its water holding capacity. A quasi 60 year cycle can also be deduced from this same figure, which is an important cycle found also in the barycentric movement. However, due to our data series length, XWT and WTC do not have the resolution to study this issue.

Finally we conclude that the climate system do have a natural component that is a long-term oscillation forced by the Sun. The source of the steady trend is more difficult to specify in this work. We assume that it is plausible to be linked to greenhouse gases increase with interannual induced variations that may be competing with those produced by solar forcing. However, it is evident that the issue depends also, for example, on the length of both the climatic and solar activity time series records, on the specific solar record that one uses, on the climate sensitivity to the low frequency variation of solar activity, and many other complications. In this respect, Li et al. (2018) for example, after detecting the role of *Rz* 11 and 22-year cycle on global temperature, could not explain its upward trend in the last decades and emphasized that global warming is mainly due to CO_2 emissions. Alternatively, for our single location study, we cannot exclude the possibility that the longest term warming trend may simply be the local manifestation of the historical environmental changes of the observing site (see discussion in Soon et al., 2015).

Through statistical analysis we tried to gain insight into the processes determining the shorter-term interannual to bidecadal variations of Tucuman climatic series with the purpose of identifying the Sun as a natural forcing, even though, ultimately, we cannot offer any direct physical arguments. However, we leave this negative result as a source of motivation for specific sun-climate insights relevant to our region until next promising adventure.

Acknowledgements

Part of this work was supported by Projects PIUNT E541 and Prestamo BID PICT 2015-0511. R.G. Cionco acknowledges the grant PID-UTN 5365TC. The efforts of W. Soon are partially funded by CERES. We thank Biblioteca Central INTA (INTA Digital: Repositorio Institucional, http://repositorio.inta.gob.ar/) for providing some of the referenced works.

References

Antico, A., Krohling, D.M., 2011. Solar motion and discharge of Parana River, South America: evidence for a link. Geophys. Res. Lett. 38, L19401. https://doi.org/10.1029/2011GL048851

Baliunas, S., Frick, P., Sokoloff, D., Soon, W., 1997. Time scales and trends in the Central England Temperature data (1659-1990): A wavelet analysis. Geophys. Res. Lett. 24, 1351-1354. https://doi.org/10.1029/97GL01184

Brandenburg, A., Mathur, S., Metcalfe, T.S., 2017. Evolution of Co-existing Long and Short Period Stellar Activity Cycles. Astrophys. J. 845, 79. https://doi.org/10.3847/1538-4357/aa7cfa

Cameron, R.H., Schussler, M., 2013. No evidence for planetary influence on solar activity. Astron. Astrophys. 557, A83. https://doi.org/10.1051/0004-6361/201321713

Charvatova, I., 2000. Can origin of the 2400-year cycle of solar activity be caused by solar inertial motion? Ann. Geophysicae 18, 399-405. https://doi.org/10.1007/s00585-000-0399-x

Cionco, R.G., Pavlov, D.A., 2018. Solar barycentric dynamics from a new solar-planetary ephemeris. Astron. Astrophys. 615, A153. https://doi.org/10.1051/0004-6361/201732349

Cionco, R.G., Pavlov, D.A., 2017. The Solar barycentric dynamics from a new solar-planetary ephemeris, PANGAEA. https://doi.org/10.1594/PANGAEA.882534

Cionco, R.G., Soon, W., 2015. A phenomenological study of the timing of solar activity minima of the last millennium through a physical modeling of the Sun-planets interaction, New Astron. 34, 164-171. https://doi.org/10.1016/j.newast.2014.07.001

Cionco, R.G., Soon, W., 2017. Short-term orbital forcing: A quasi-review and a reappraisal of realistic boundary conditions for climate modeling, Earth-Sci- Rev. 166, 206-222. https://doi.org/10.1016/j.earscirev.2017.01.013

Cionco, R.G., Abuin, P., 2016. On planetary torque signals and sub-decadal frequencies in the discharges of large rivers, Adv. Space Res. 57, 1411-1425. https://doi.org/10.1016/j.asr.2015.05.046

Cionco, R.G., Compagnucci, R.H., 2012. Dynamical characterization of the last prolonged solar minima. Adv. Space Res. 50, 1434–1444. https://doi.org/10.1016/j.asr.2012.07.013

Coddington, O., Lean, J.L., Pilewskie, P., Snow, M., Lindholm, D., 2015. A solar irradiance climate data record, B. Am. Meteorol. Soc. 97, 1265–1282. https://doi.org/10.1175/BAMS-D-14-00265.1

Elias, A.G., Zossi, M., 2006. The quasi-decadal modulation of running correlations involving the QBO, J. Atmos. Solar-Terr. Phys. 68, 1980–1986. https://doi.org/10.1016/j.jastp.2006.08.003

Gil-Alana, L.A., Yaya, O.S.,. Shittuc, O.I , 2014. Global temperatures and sunspot numbers. Are they related?, Physica A 396, 42–50. https://doi.org/10.1016/j.physa.2013.10.043

Granger, C.W.J., 1969. Investigating causal relations by econometrics models and crossspectral methods. Econometrica, 37, 424–438. https://doi.org/10.2307/1912791

Grinsted, A., Moore, J., Jevrejeva, S., 2004. Application of the cross wavelet transform and wavelet coherence to geophysical time series. Nonlin. Processes Geophys. 11, 561–566. https://doi.org/10.5194/npg-11-561-2004

Heredia, T., Elias, A.G., 2013. A study on possible solar and geomagnetic effects on the precipitation over northwestern Argentina. Adv. Space Res. 51,1883–1892. https://doi.org/10.1016/j.asr.2013.01.020

Holm, S., 2014. On the alleged coherence between the global temperature and the sun's movement. J. Atmos. Solar-Terr. Phys. 110, 23–27. https://doi.org/10.1016/j.jastp.2014.01.014

Holm, S., 2015. Prudence in estimating coherence between planetary, solar and climate oscillations, Astrophysics and Space Science, 357. https://doi.org/10.1007/s10509-015-2334-3

IPCC, 2014. Climate Change 2014: Synthesis Report. Contribution of Working Groups I, II and III to the Fifth Assessment Report of the Intergovernmental Panel on Climate Change [Core Writing Team, R.K. Pachauri and L.A. Meyer (eds.)]. IPCC, Geneva, Switzerland, 151 pp.

Jones, P.D., Lister, D.H., Osborn, T.J., Harpham, C., Salmon, M., Morice, C.P., 2012. Hemispheric and large-scale land surface air temperature variations: an extensive revision and an update to 2010. J. Geophys. Res. 117, D05127. http://doi.org/10.1029/2011JD017139

Jose, P.D., 1965. Sun's motion and sunspots. Astron. J. 70, 193–200. http://doi.org/10.1086/109714

Kennedy J.J., Rayner, N.A., Smith, R.O., Saunby, M., Parker, D.E., 2011a. Reassessing biases and other uncertainties in sea-surface temperature observations since 1850 part 1: measurement and sampling errors. J. Geophys. Res., 116, D14103. http://doi.org/10.1029/2010JD015218

Kennedy J.J., Rayner, N.A., Smith, R.O., Saunby, M., Parker, D.E., 2011b. Reassessing biases and other uncertainties in sea-surface temperature observations since 1850 part 2: biases and homogenisation. J. Geophys. Res., 116, D14104. http://doi.org/10.1029/2010JD015220

Kenning, W., 1963. Las lluvias en San Migue de Tucuman, Argentina (1885/85-1961/62), IDIA (Journal of the Instituto Nacional de Tecnologia Agropecuaria, INTA), 189, 19-27.

Kirkby, J.. 2007. Cosmic rays and clouds, Surveys in Geophysics 28, 333–375. http://doi.org/10.1007/s10712-008-9030-6

Kristoufek , L., 2017. Has global warming modified the relationship between sunspot numbers and global temperatures?, Phyisca A, 468, 351-358. https://doi.org/10.1016/j.physa.2016.10.089

Li, Z., Yue, J., Xiang, Y., Chen, J., Bian, Y., Chen, H., 2018. Multiresolution Analysis of the Relationship of Solar Activity, Global Temperatures, and Global Warming, Advances in Meteorology, ID 2078057. https://doi.org/10.1155/2018/2078057

Leal-Silva, M.C., Velasco Herrera, V.M., 2012. Solar forcing on the ice winter severity index in the western Baltic region. J. Atmos. Solar-Terr. Phys. 89, 98–109. https://doi.org/10.1016/j.jastp.2012.08.010

Matthes, K., Funke, B., Andersson, M.E., Barnard, L., Beer , J., Charbonneau, P., Clilverd, M.A., et al., 2017. Solar forcing for CMIP6 (v3.2). Geosci. Model Dev., 10, 2247–2302. https://doi.org/10.5194/gmd-10-2247-2017

McCracken, K.G., Beer, J., Steinhilber, F., 2014. Evidence for Planetary Forcing of the Cosmic Ray Intensity and Solar Activity Throughout the Past 9400 Years, Solar Physics, 289, 3207-3229. https://doi.org/10.1007/s11207-014-0510-1

McCrann, M., Russell, J., Ionescu, D., Mainali, B., 2018. Sea levels in a Changing Climate, Int. Jour. of GEOMATE, 14, 24-30. http://doi.org/10.21660/2018.43.3522

Mendoza, V.M., Mendoza, B., Garduño, R., Villanueva, E.E., Adem, J., 2016. Solar activity cloudiness effect on NH warming for 1980–2095, Advances in Space Research, 57, 1373-1390. https://doi.org/10.1016/j.asr.2015.11.024

Minetti, J.L., 1991. Estudio de las singularidades climáticas en series de temperaturas del noroeste argentino. Facultad de Ciencias Exactas y Naturales. Universidad de Buenos Aires. (Available at http://digital.bl.fcen.uba.ar/Download/Tesis/Tesis_2410_Minetti.pdf)

Minetti, J.L., Vargas, W.M., 1997. Trends and jumps in the annual precipitation in South America, south of the 15°S, Atmosfera, 11, 205-221. (Available in http://www.redalyc.org/articulo.oa?id=56511402)

Okhlopkov, V.P., 2016. The gravitational influence of Venus, the Earth, and Jupiter on the 11-year cycle of solar activity. Moscow University Physics Bulletin, 71, 440–446. https://doi.org/10.3103/S0027134916040159

Priest, E., 2011. The nature and significance of solar minima, Proceedings of the International Astronomical Union, 7(S286), 3-14. https://doi.org/10.1017/S1743921312004577

Russell, C.T., Luhmann, J.G., Strangeway, R.J., 2016. Space Physics: An Introduction, Cambridge University Press, United Kingdom.

Scafetta, N., West, B., 2007. Phenomenological reconstructions of the solar signature in the NH surface temperature records since 1600. J. Geophys. Res. 112, D24S03. https://doi.org/10.1029/2007JD008437

Scafetta, N., 2010. Empirical evidence for a celestial origin of the climate oscillations and its implications. J. Atmos. Solar Terr. Phys. 72, 951–970. https://doi.org/10.1016/j.jastp.2010.04.015

Scafetta, N., 2012. Testing an astronomically based decadal-scale empirical harmonic climate model versus the IPCC (2007) general circulation climate models. J. Atmos. Sol. Terr. Phys. 80, 124–137. https://doi.org/10.1016/j.jastp.2011.12.005

Scafetta, N., 2014. Discussion on the spectral coherence between planetary, solar and climate oscillations: a reply to some critiques. Astrophys. Space Sci., 354, 275–299. https://doi.org/10.1007/s10509-014-2111-8

Scafetta, N., 2016. High resolution coherence analysis between planetary and climate oscillations. Adv. Space Res. 57, 2121–2135. https://doi.org/10.1016/j.asr.2016.02.029

Scafetta, N., 2018. Reply on Comment on "High resolution coherence analysis between planetary and climate oscillations" by S. Holm. Adv. Space Res. 62, 334-342. https://doi.org/10.1016/j.asr.2018.05.014

Seluchi, M.E., Saulo, A.C., Nicolini, M., Satyamurty, P., 2003. The Northwestern Argentinean Low: a study of two typical events. Mon. Weather Rev. 131, 2361–2378. https://doi.org/10.1175/1520-0493(2003)131<2361:TNALAS>2.0.CO;2

Sfica, L., Iordache, J., Voiculescu, M., 2018. Solar signal on regional scale: A study of possible solar impact upon Romania's climate. J. Atmos. Solar-Terr. Phys. 177, 257–265. https://doi.org/10.1016/j.jastp.2017.09.015

Soon, W.H., 2009. Solar Arctic-mediated climate variation on multidecadal to centennial timescales: Empirical evidence, mechanistic explanation and testable consequences. Physical Geography, 30, 144-184. https://doi.org/10.2747/0272-3646.30.2.144

Soon, W., Velasco Herrera, V.M., Selvaraj, K., Traversi, R., Usoskin, I., Chen, C.T.A., Lou, J.-Y., Kao, S.-J., Carter, R.M., Pipin, V., Severi, M., Becagli, S., 2014. A review of Holocene solar-linked climatic variation on centennial to millennial timescales: Physical processes, interpretative frameworks and a new multiple cross-wavelet transform algorithm. Earth-Science Rev. 134, 1-15. https://doi.org/10.1016/j.earscirev.2014.03.003

Soon, W., Connolly, R., Connolly, M., 2015. Re-evaluating the role of solar variability on Northern Hemisphere temperature trends since the 19th century. Earth-Science Rev. 150, 409-452. https://doi.org/10.1016/j.earscirev.2015.08.010

Stefani, F., Giesecke, A., Weier, T., 2019. A model of a tidally synchronized solar dynamo. Solar Physics 294, article 60 (27 pp.).

Sun, W., Wang, J., Chen, J.R., Wang, Y., Yu, G.M., Xu, X.H., 2017. Contrast analysis between the trajectory of the planetary system and the periodicity of solar activity. Ann. Geophysicae 35, 659–669. https://doi.org/10.5194/angeo-35-659-2017

Tlatov, A.G., 2013. Reversals of Gnevyshev-Ohl rule. The Astrophysical Journal Letters 772, L30. https://doi.org/10.1088/2041-8205/772/2/L30

Torrence, C., Compo, G.P., 1998. A practical guide to wavelet analysis. Bull. Am. Met. Soc. 79, 61–78. https://doi.org/10.1175/1520-0477(1998)079<0061:APGTWA>2.0.CO;2

Usoskin, I.G., Gallet, Y., Lopes, F., Kovaltsov, G.A., Hulot, G., 2016. Solar activity during the Holocene: the Hallstatt cycle and its consequence for grand minima and maxima. Astronomy and Astrophysics, 587, A150. https://doi.org/10.1051/0004-6361/201527295

Wang, G., Yang, P., Zhou, X., 2017. Identification of the driving forces of climate change using the longest instrumental temperature record. Scientific Reports, 7, 46091. https://doi.org/10.1038/srep46091

Wiskot, L., 2003. Estimating Driving Forces of Nonstationary Time Series with Slow Feature Analysis, arXiv:cond-mat/0312317.

Yndestad, H., Solheim, J.E., 2017. The influence of solar system oscillation on the variability of the total solar irradiance. New Astronomy, 51, 135-152. https://doi.org/10.1016/j.newast.2016.08.020

Zanchettin, D., Rubino, A., Traverso, P., Tomasino, M., 2008. Impact of variations in solar activity on hydrological decadal patterns in northern Italy. J. Geophys. Res., 113, 12102. https://doi.org/10.1029/2007JD009157

Zolotova, N.V., Ponyavin, D.I., 2015. The Gnevyshev-Ohl rule and its violations. Geomagnetism and Aeronomy 55, 902-906. https://doi.org/10.1134/S0016793215070300

Tables

Table 1. Climatic parameters' variation due to the long term trend along the 130-year period between 1889 and 2018 obtained from a quadratic fit (3rd column), and variation along half the 20-year cycle obtained from an FFT (5th column), together with the corresponding variations per year (2nd and 4th columns). ±: variation is positive (along the rising phase of the cycle) and negative (along the decreasing phase of the cycle). SH: Southern Hemisphere, NH: Northern Hemisphere

Climatic parameter	**σ**	**Long-term trend**		**20-year oscillation**	
		Variation in 130 years	**Variation per year**	**Variation in half a cycle**	**Variation per year**
Tucuman precipitation	213 mm	148 mm	1 mm	±120 mm	±12 mm
Tucuman temperature	0.621°	0.57°	0.004°	±0.50°	±0.050°
NH land	0.220°	1.30°	0.010°	±0.08°	±0.008°
NH sea	0.152°	0.80°	0.006°	±0.06°	±0.006°
SH land	0.156°	1.09°	0.008°	±0.06°	±0.006°
SH sea	0.107°	0.85°	0.007°	±0.10°	±0.010°

Table 2. Correlation coefficients between 11-year running mean of annual climatic and solar series. 95% confidence level: $r_c \geq 0.52$

Climatic parameter	*r*	*L*	d*L*/d*t*	*Rz*	TSI
Tucuman precipitation	0.40	0.38	0.03	019	0.19
Tucuman temperature	-0.08	-0.03	-1.13	-0.32	-0.36
SH land	0.09	0.16	-0.07	-0.28	-0.33
SH sea	0.39	0.36	0.10	0.38	0.29
NH land	0.02	0.09	-0.09	-0.16	-0.18
NH sea	0.04	0.07	-0.08	0.14	0.10

Figures

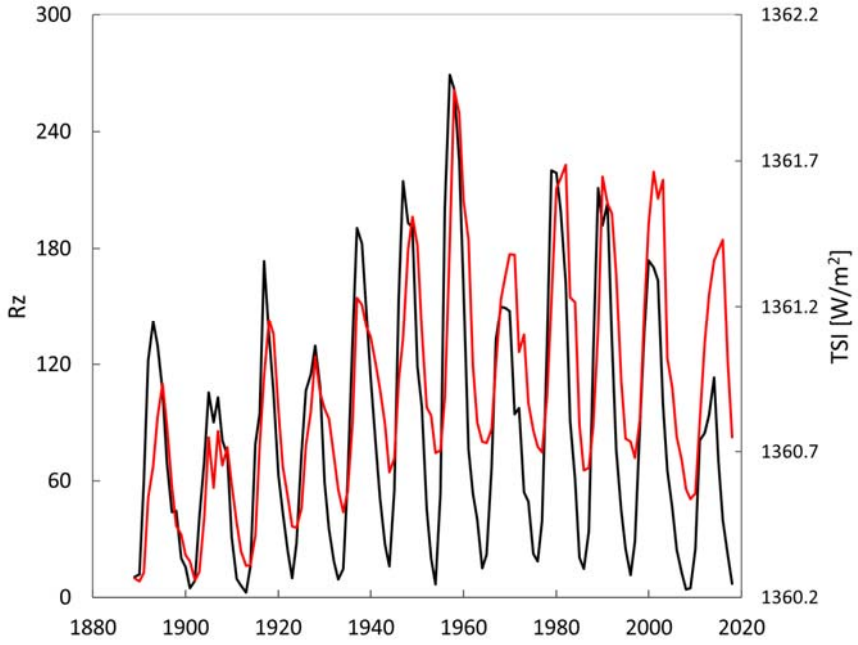

(a)

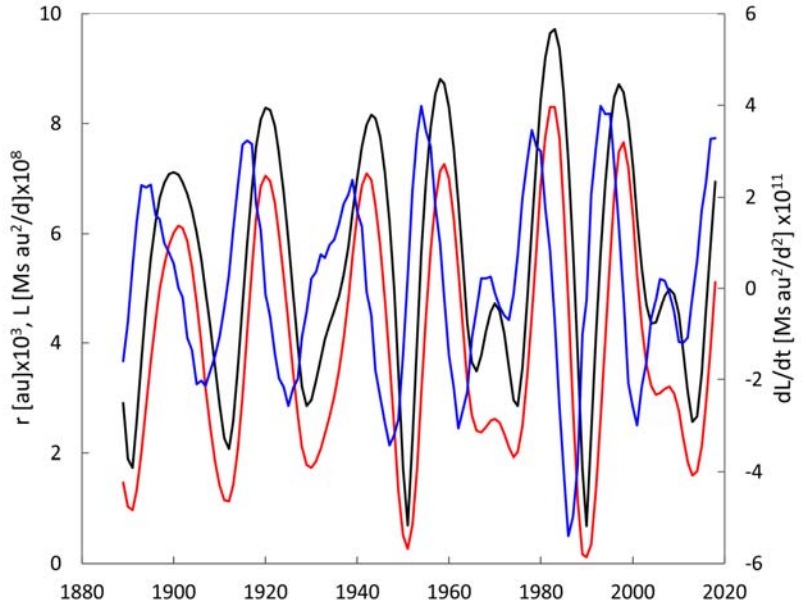

(b)

Figure 1. (a) Total Solar Irradiance TSI (red) [W/m^2] and sunspot number Rz (black); (b) the magnitude of the solar barycentric position, *r* (black) x10^3 [au], the modulus of the solar orbital angular momentum *L* (red) x10^8 [Ms au/d], and solar "torque" d*L*/d*t* (blue) x10^{11} [Ms au/d^2] . Period 1889-2018. Ms: 1.989x10^{30}kg; au: 149597870700 m; d: 86400s.

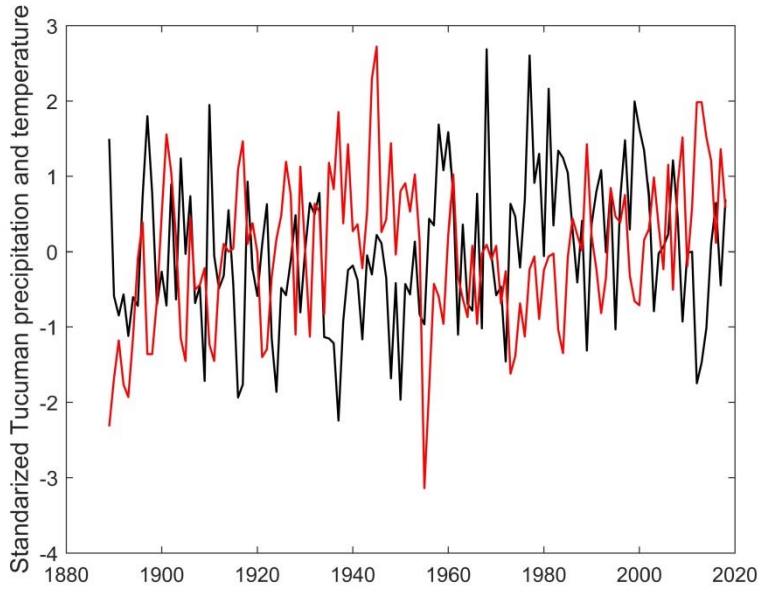

(a)

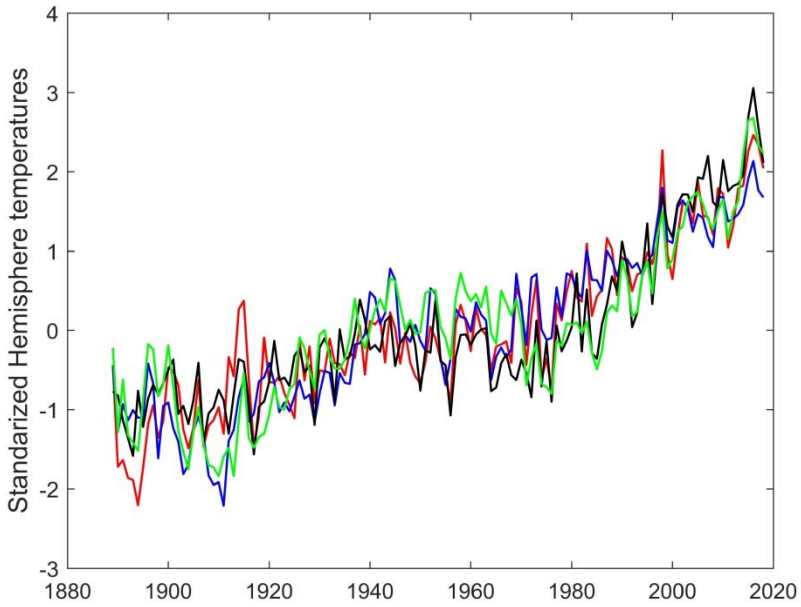

(b)

Figure 2. (a) Annual mean temperature (red) and total precipitation (black) over Tucuman. (b) Hemispheric annual mean temperature: SH land (red), SH sea (blue), NH land (black), and NH sea (green). All series are standardized, and shown for the period 1889-2018.

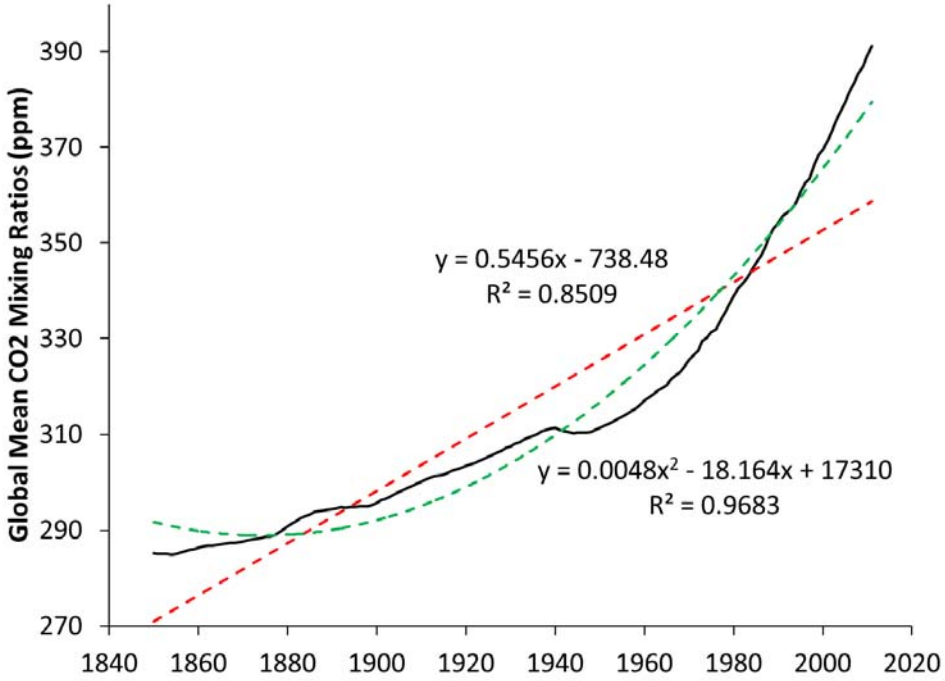

Figure 3. Global mean CO2 mixing ratios (ppm) obtained from the Goddard Institute for Space Studies (GISS) (data available at https://data.giss.nasa.gov/modelforce/ghgases/Fig1A.ext.txt)

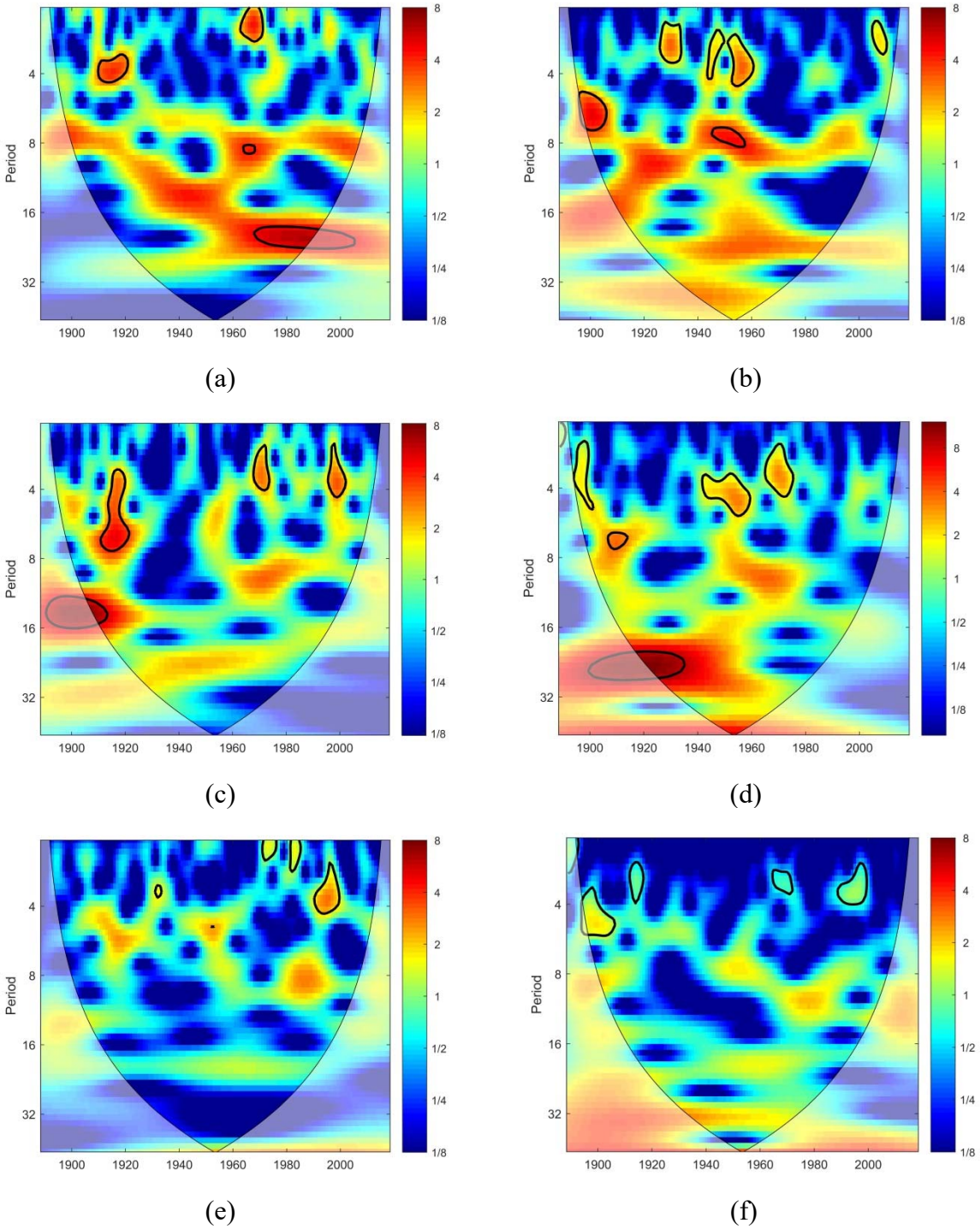

Figure 4. Wavelet transform of (a) total annual precipitation over Tucuman, (b) Tucuman annual mean temperature, and annual mean temperatures (c) NH land, (d) NH sea, (e) SH land, (f) SH sea. Period 1889-2018. (Thick black contour: 95% confidence level; lighter black line: cone of influence, COI)

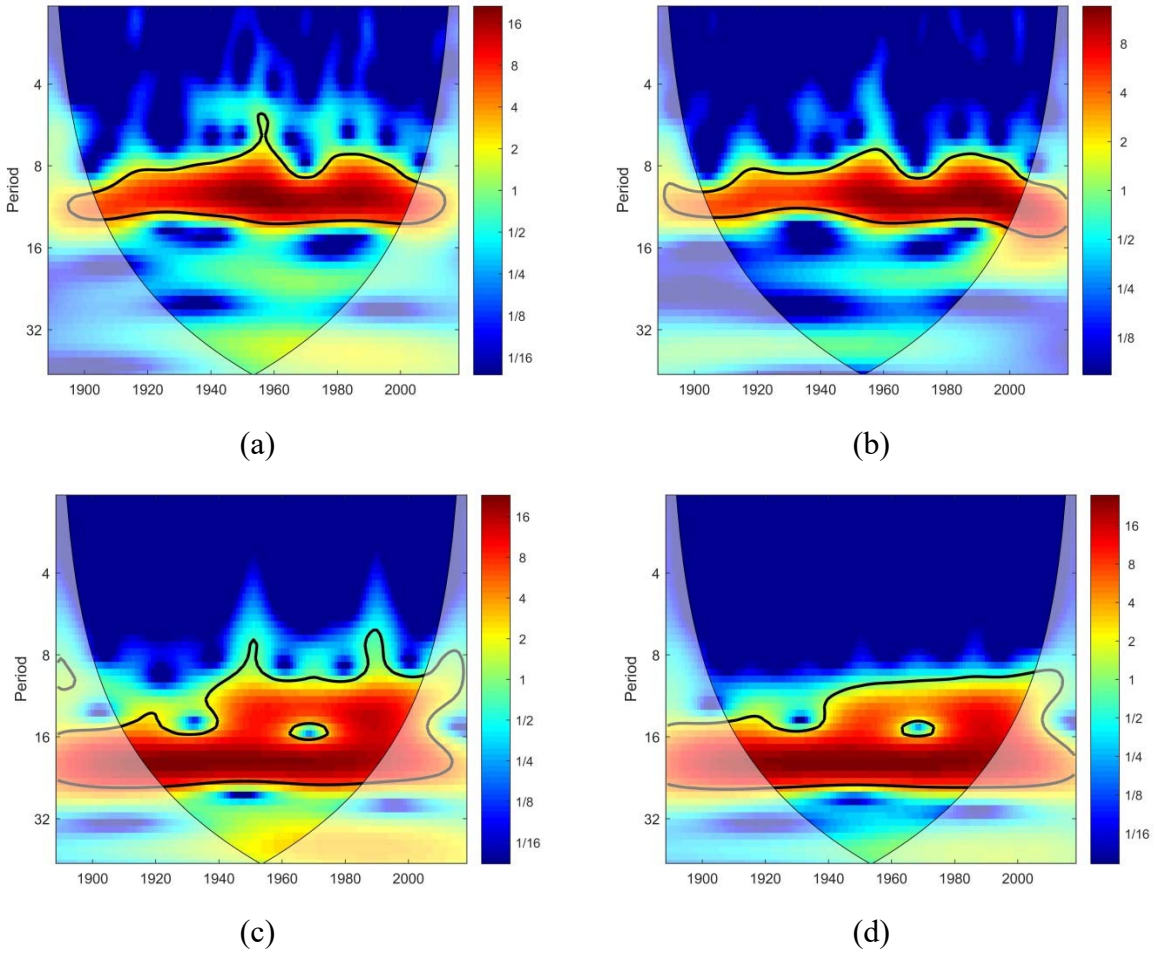

Figure 5. Wavelet transform of annual mean (a) sunspot number, *Rz*, (b) total solar irradiance, TSI, (c) the magnitude of the solar barycentric position, *r*, and (d) the modulus of the solar orbital angular momentum, *L*. Period 1889-2018. (Thick black contour: 95% confidence level; lighter black line: cone of influence, COI)

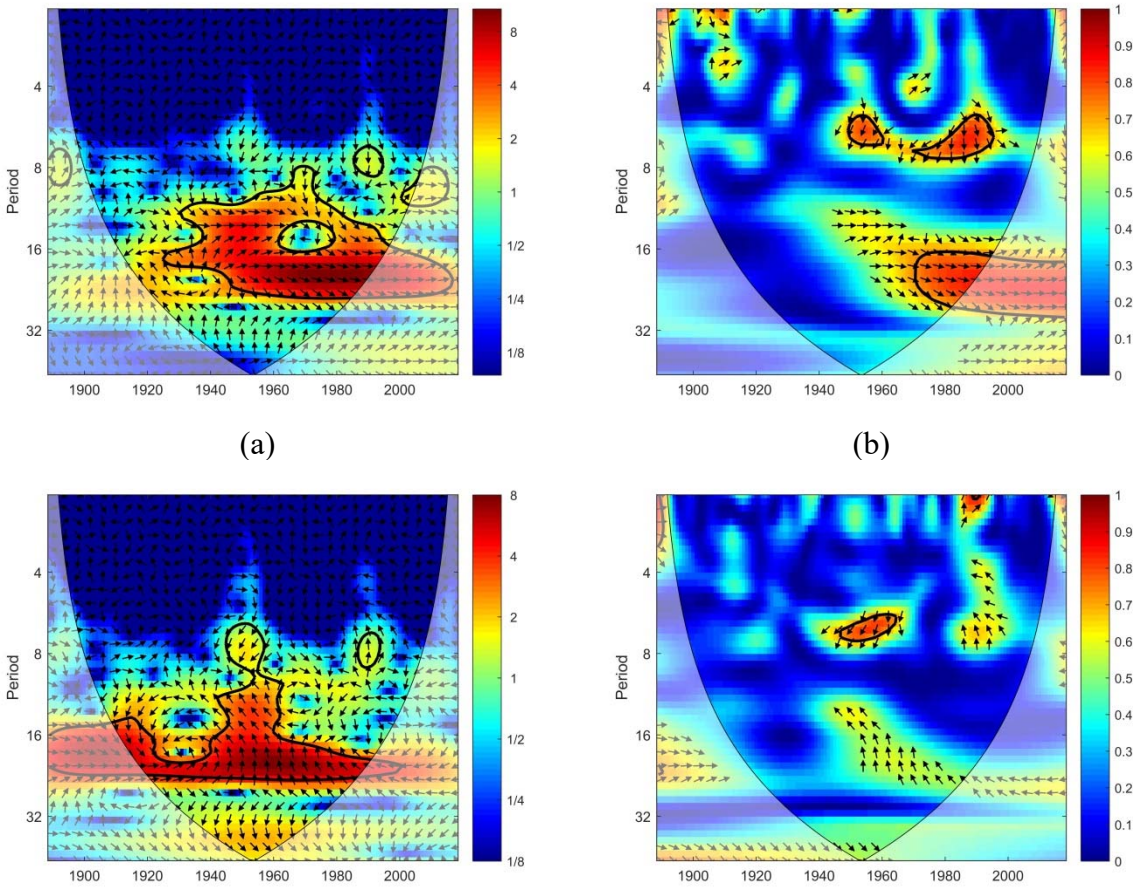

Figure 6. Cross wavelet spectrum XWT (left panels) and wavelet coherence WTC (right panels) for the period 1889-2018, between the solar barycentric distance, *r*, and (a,b) Tucuman total annual precipitation and (c,d) Tucuman mean annual temperature. Both series detrended with a quadratic fit. (Thick black contour: 95% confidence level; lighter black line: cone of influence, COI)

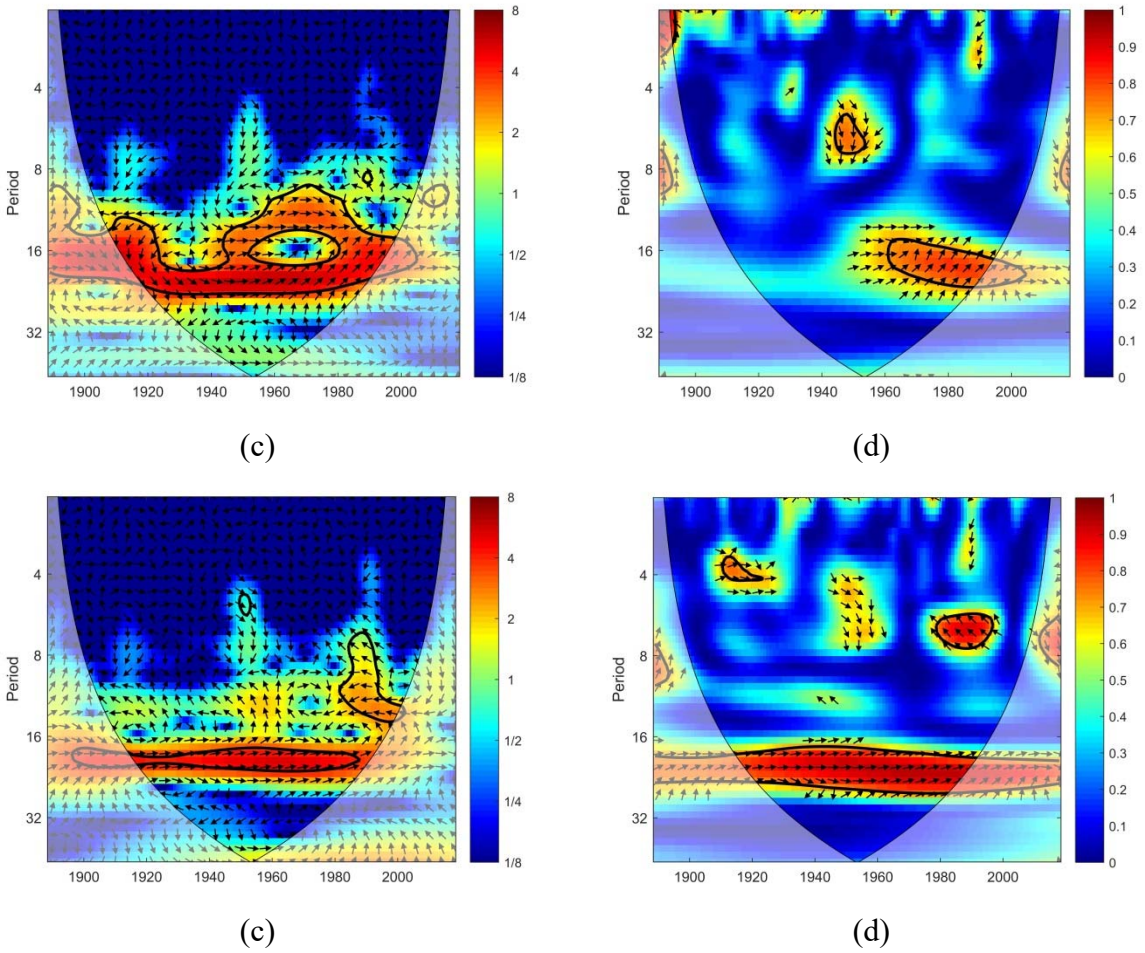

Figure 7. Cross wavelet spectrum XWT (left panels) and wavelet coherence WTC (right panels) for the period 1889-2018, between solar barycentric distance, *r*, and (a,b) SH land temperature and (c,d) NH land temperature. Both series detrended with quadratic fit. (Thick black contour: 95% confidence level; lighter black line: cone of influence, COI)

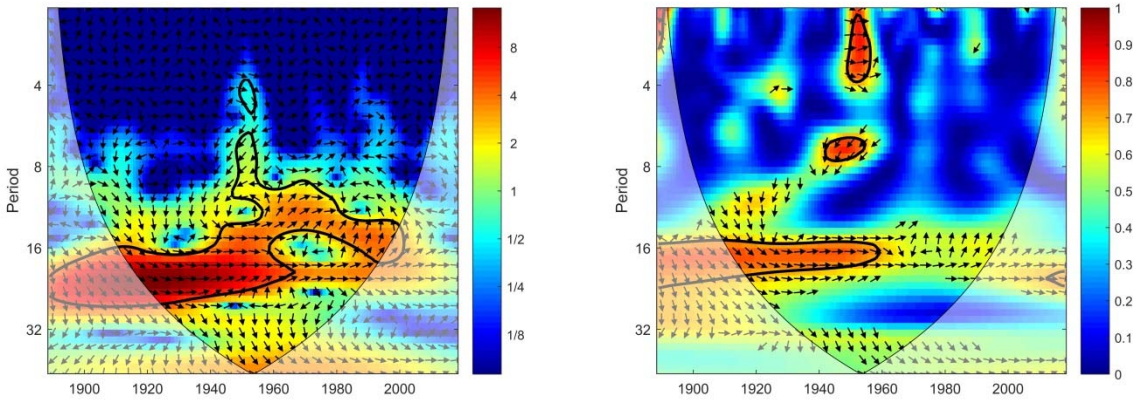

(c) (d)

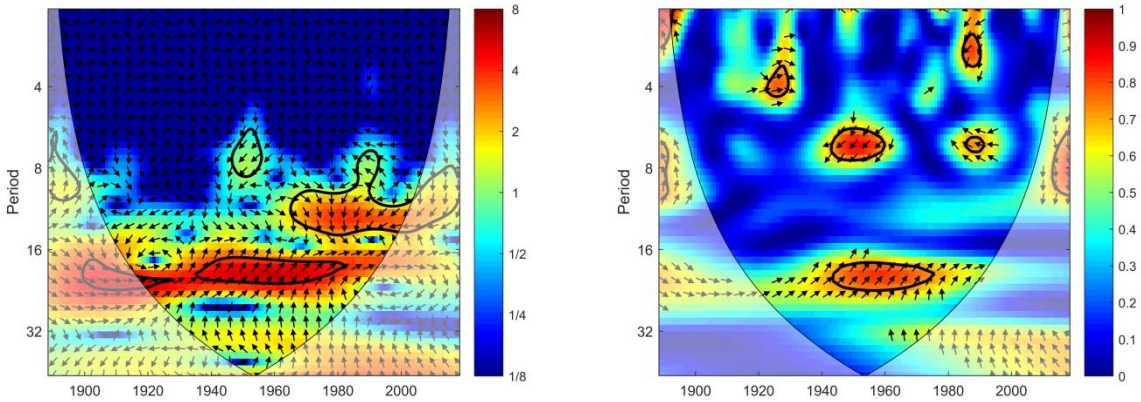

(c) (d)

Figure 8. Cross wavelet spectrum XWT (left panels) and wavelet coherence WTC (right panels) for the period 1889-2018, between solar barycentric distance, *r*, and (a,b) SH sea temperature and (c,d) NH sea temperature. Both series detrended with quadratic fit. (Thick black contour: 95% confidence level; lighter black line: cone of influence, COI)

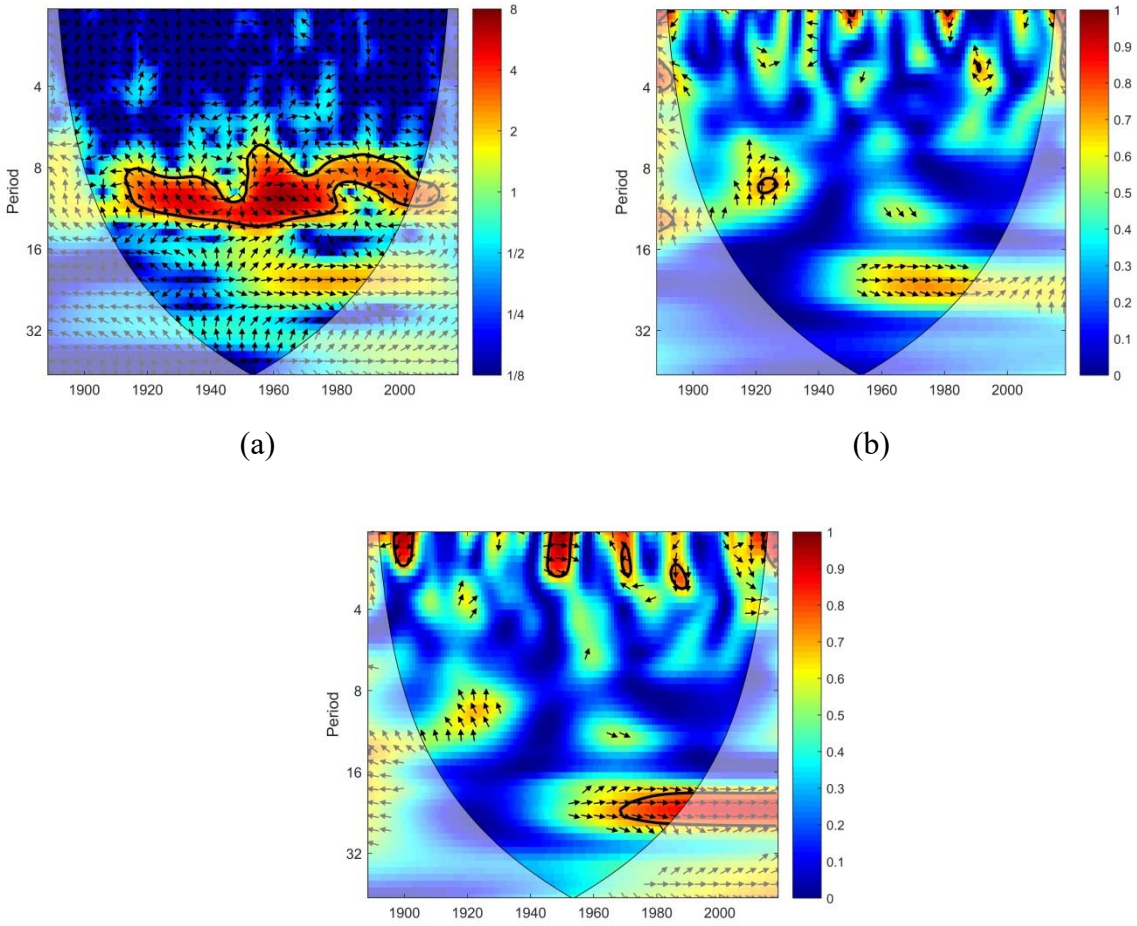

(a) (b)

(c)

Figure 9. (a) Cross wavelet spectrum XWT and (b) wavelet coherence WTC for the period 1889-2018, between TSI and Tucuman total annual precipitation. (c) WTC between *Rz* and Tucuman annual precipitation. Precipitation series detrended with quadratic fit. (Thick black contour: 95% confidence level; lighter black line: cone of influence, COI)

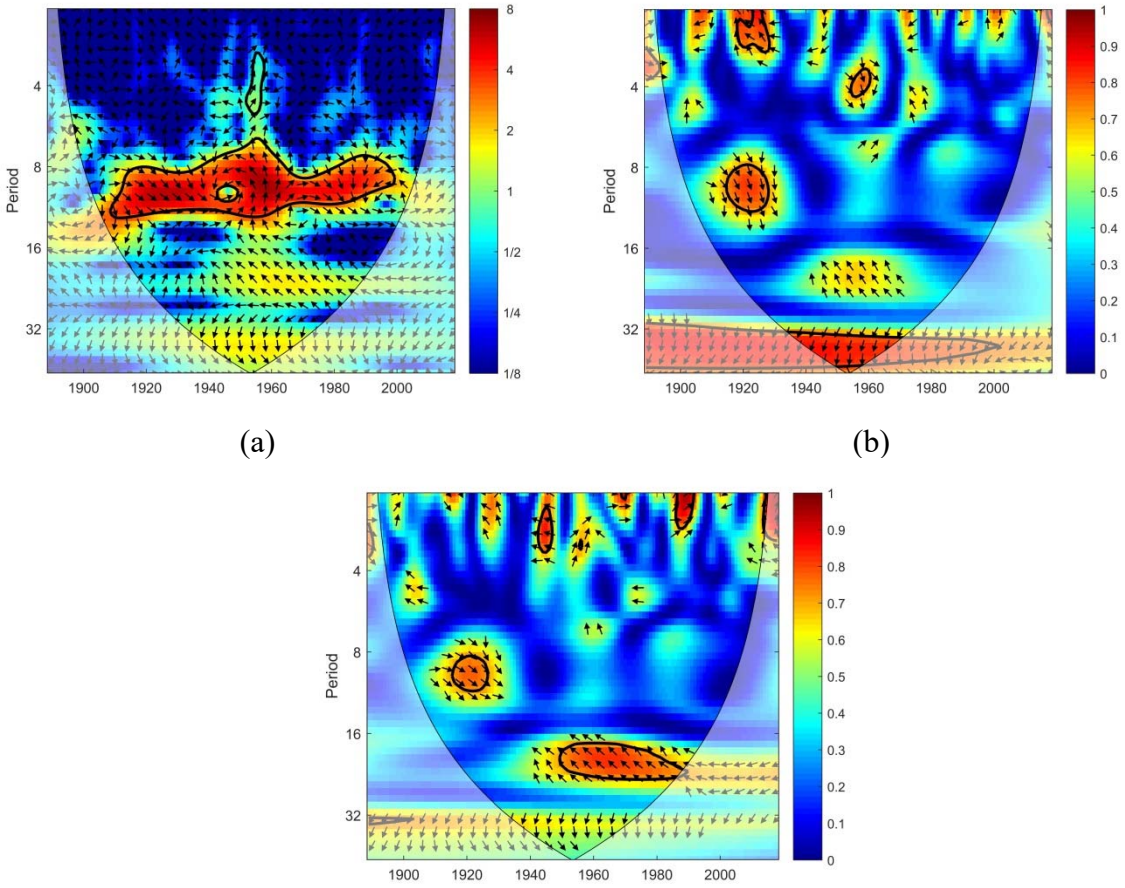

Figure 10. (a) Cross wavelet spectrum XWT and (b) wavelet coherence WTC for the period 1889-2018, between TSI and Tucuman mean temperature. (c) WTC between *Rz* and Tucuman mean temperature. Temperature series detrended with quadratic fit. (Thick black contour: 95% confidence level; lighter black line: cone of influence, COI)

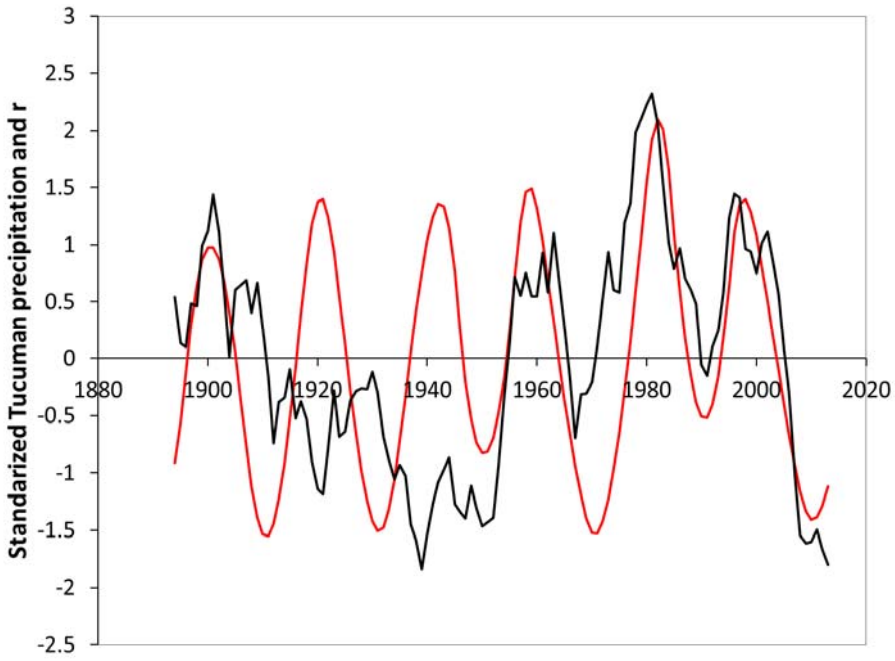

Figure 11. Tucuman total annual precipitation (black) and between the solar barycentric distance *r* (red) after an 11-year running mean. Both series are standardized.

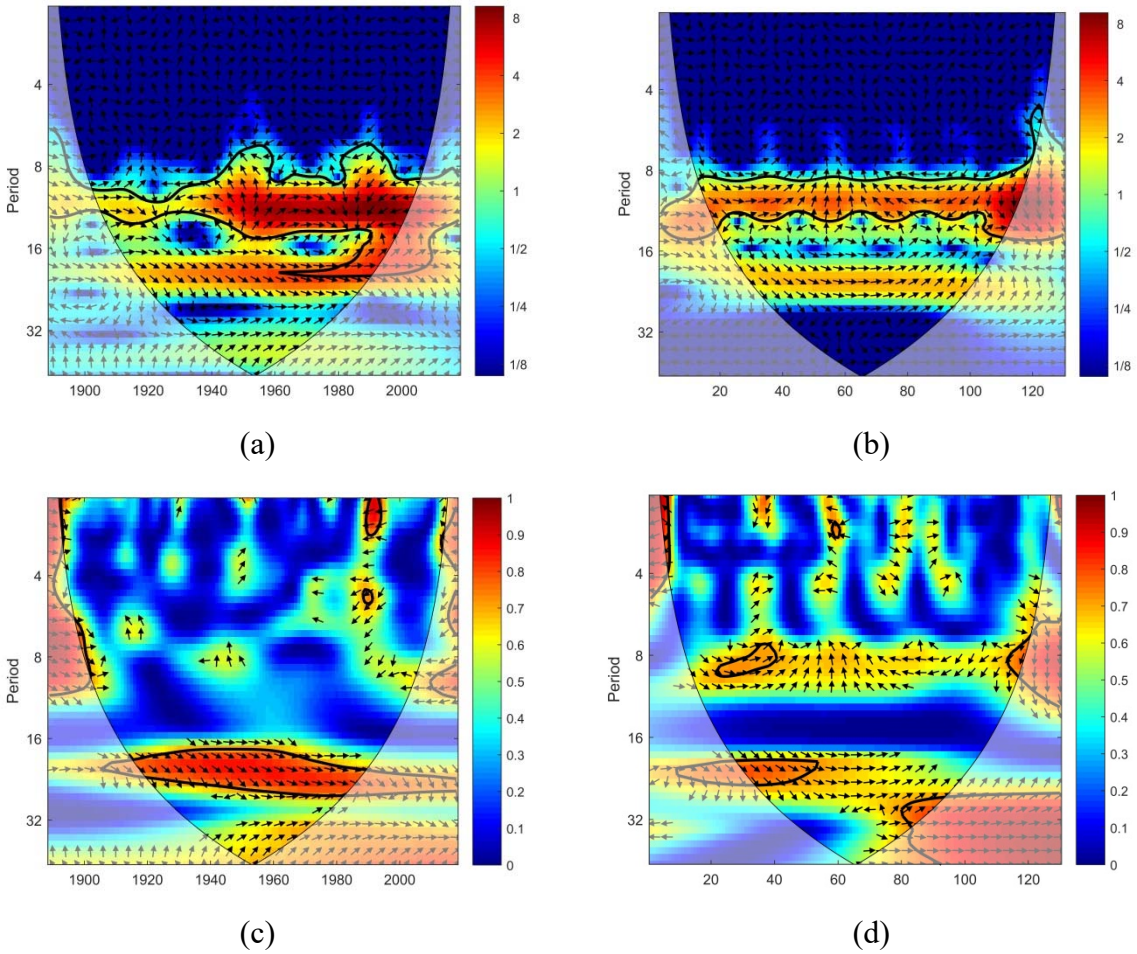

Figure 12. Cross wavelet spectrum XWT (upper panels) and wavelet coherence WTC (lower panels) for the period 1889-2018, between (a,c) TSI and *r*, and (b,d) artificial series: one with a quasi-decadal cycle (11-year periodicity) of alternating maxima and asymmetric rise and falling time, and the other with a bi-decadal cycle of asymmetric rise and falling time. (Thick black contour: 95% confidence level; lighter black line: cone of influence, COI)